

See discussions, stats, and author profiles for this publication at: <https://www.researchgate.net/publication/231524691>

# “Bare” Iron Methoxide Cation: A Simple Model To Probe the Mechanism of $\beta$ -Hydrogen Transfer in Organometallic Compounds

ARTICLE *in* JOURNAL OF THE AMERICAN CHEMICAL SOCIETY · MAY 1996

Impact Factor: 12.11 · DOI: 10.1021/ja953039q

---

CITATIONS

72

---

READS

6

5 AUTHORS, INCLUDING:



P. B. Armentrout

University of Utah

492 PUBLICATIONS 20,531 CITATIONS

SEE PROFILE

# “Bare” Iron Methoxide Cation: A Simple Model To Probe the Mechanism of $\beta$ -Hydrogen Transfer in Organometallic Compounds

Andreas Fiedler,<sup>†</sup> Detlef Schröder,<sup>\*,†</sup> Helmut Schwarz,<sup>†</sup> Brenda L. Tjelta,<sup>‡</sup> and P. B. Armentrout<sup>\*,‡</sup>

Contribution from the Institut für Organische Chemie, Technische Universität Berlin, D-10623 Berlin, Germany, and Department of Chemistry, University of Utah, Salt Lake City, Utah 84112

Received September 5, 1995<sup>⊗</sup>

**Abstract:** Iron methoxide cation,  $\text{Fe}(\text{OCH}_3)^+$  (**1**), and its tautomer, the formaldehyde complex of the iron hydride cation,  $\text{HFe}(\text{OCH}_2)^+$  (**2**), have been examined in combined mass spectrometric and computational studies. Although the experimental methods used for ion generation yield two isomers, largely because intermolecular isomerization is facile, differentiation of them is straightforward.  $\text{Fe}(\text{OCH}_3)^+$  corresponds to the global minimum of the  $[\text{Fe}, \text{C}, \text{H}_3, \text{O}]^+$  potential-energy hypersurface with an experimentally determined bond-dissociation energy of  $69 \pm 2$  kcal/mol for the  $\text{Fe}^+ - \text{OCH}_3$  bond. In the gas phase,  $\text{Fe}(\text{OCH}_3)^+$  can isomerize via a  $\beta$ -hydrogen transfer to  $\text{HFe}(\text{OCH}_2)^+$ , which is experimentally found to be  $15 \pm 4$  kcal/mol less stable than  $\text{Fe}(\text{OCH}_3)^+$ . The experiments suggest and the calculations predict that the two isomers are separated by a significant activation barrier. According to the calculations both species exhibit quintet ground states and the transition structure associated with their interconversion on the quintet potential-energy hypersurface is 37 kcal/mol above  $\text{Fe}(\text{OCH}_3)^+$ . Consideration of the excited triplet surface indicates that the barrier for the  $\beta$ -hydrogen transfer connecting both isomers may be lowered substantially by additional ligands. Moreover, in the complexes  $\text{Fe}(\text{L})(\text{OCH}_3)^+$  ( $\text{L} = \text{C}_2\text{H}_4, \text{CH}_2\text{O}$ ) direct H-transfer from the  $\text{OCH}_3$  ligand to L may occur without involving an iron hydride as an intermediate.

## Introduction

$\beta$ -Hydrogen transfer represents the most important isomerization reaction in organometallic chemistry. Many experimental and theoretical attempts have been made to understand the function of the metal center for  $\beta$ -hydrogen transfers in economically and technically important processes such as olefin polymerization, hydroformylation, and the reduction of aldehydes.<sup>1</sup>

For an understanding of the basic principles of  $\beta$ -hydrogen transfer, knowledge of the electronic and geometric structures of the intermediates and transition structures is a prerequisite. Metal alkoxides<sup>2</sup> are involved in a series of important chemical transformations, including the Meerwein–Ponndorf–Verley reduction of aldehydes and ketones and the corresponding Oppenauer oxidation of primary and secondary alcohols.<sup>3</sup> For transition-metal alkoxides,  $\beta$ -hydrogen transfer is believed to be one of the most important factors in their chemical reactivity; however, direct experimental evidence aimed at elucidating details of the mechanism of  $\beta$ -hydrogen transfer is relatively scarce.<sup>4</sup> Based on density functional theory (DFT), Versluis and Ziegler<sup>5</sup> carried out theoretical calculations on the singlet potential-energy hypersurface for the  $\beta$ -hydrogen transfer in the

18-electron complex of formaldehyde with hydrido cobalt tricarbonyl,  $\text{HCo}(\text{CH}_2\text{O})(\text{CO})_3$ . Their most interesting finding was that  $\beta$ -hydrogen transfer is accompanied by only a modest barrier of ca. 5 kcal/mol to yield a  $\beta$ -agostic cobalt methoxide; however, the following step from the  $\beta$ -agostic structure to the classical methoxy complex  $(\text{CH}_3\text{O})\text{Co}(\text{CO})_3$  is hampered by a substantial barrier on the order of 80 kcal/mol. These authors pointed out that this high barrier may be reduced in the liquid phase due to additional incoming ligands, which could then allow for a  $\beta$ -hydrogen transfer at thermal energies. In addition, there exists experimental<sup>6</sup> and theoretical<sup>7</sup> support for believing that the four-centered intermediates of  $\beta$ -hydrogen transfer, which correspond to transition structures from the classical point of view, may be minima on the potential-energy hypersurface due to agostic stabilization.

Gas-phase experiments are attractive tools for the examination of intrinsic reactivities of transition-metal compounds without complicating effects due to aggregation, counterions, solvents, etc. Therefore, these studies allow not only for the determination of the thermodynamic properties but also for the elaboration of kinetic and energetic parameters that influence reaction mechanisms, selectivities, and regiochemistry.<sup>8</sup> In cationic, transition-metal-containing systems,  $\beta$ -hydrogen migrations have been observed to occur very efficiently and also reversibly.<sup>9</sup> These findings point to small barriers for  $\beta$ -H transfer in open-shell compounds,<sup>10</sup> although in some cases,

<sup>†</sup> Technische Universität Berlin.

<sup>‡</sup> University of Utah.

<sup>⊗</sup> Abstract published in *Advance ACS Abstracts*, May 1, 1996.

(1) Elschenbroich, C.; Salzer, A. *Organometallchemie*, Teubner: Stuttgart, 1989.

(2) Bradley, D. C.; Mehrota, R. C.; Gaur, D. P. *Metal Alkoxides*, Academic Press: London, 1978.

(3) (a) Meerwein, H.; Schmidt, R. *Liebigs Ann.* **1925**, 444, 221. (b) Verley, A. *Bull. Soc. Chem. Fr.* **1925**, 37, 537. (c) Ponndorf, W. *Z. Angew. Chem.* **1926**, 39, 138. (d) Oppenauer, R. V. *Recl. Trav. Chim.* **1937**, 56, 137.

(4) For a recent mechanistic study and numerous references, see: Blum, O.; Milstein, D. *J. Am. Chem. Soc.* **1995**, 117, 4582.

(5) Versluis, L.; Ziegler, T. *J. Am. Chem. Soc.* **1990**, 112, 6763.

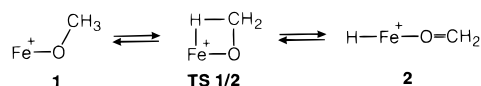
(6) (a) Brookhart, M.; Lincoln, D. M.; Volpe, A. F., Jr.; Schmidt, G. F. *Organometallics* **1989**, 8, 1212. (b) Brookhart, M.; Lincoln, D. M.; Bennett, M. A.; Pelling, S. *J. Am. Chem. Soc.* **1990**, 112, 2691. (c) Brookhart, M.; Volpe, A. F., Jr.; Lincoln, D. M.; Horváth, I. T.; Millar, J. M. *J. Am. Chem. Soc.* **1990**, 112, 5634.

(7) Versluis, L.; Ziegler, T.; Fan, L. *Inorg. Chem.* **1990**, 29, 4530.

(8) Eller, K.; Schwarz, H. *Chem. Rev.* **1991**, 91, 1121.

(9) Houriet, R.; Halle, L. F.; Beauchamp, J. L. *Organometallics* **1983**, 2, 1818.

## Scheme 1



$\beta$ -hydrogen transfer was shown to participate in the rate-determining step of C–H bond activation, e.g. in the remote functionalization of nitriles by bare  $\text{Fe}^+$  cations.<sup>11</sup>

Here, we discuss the structures and energetics of iron methoxide  $\text{Fe}(\text{OCH}_3)^+$  (**1**), its tautomer  $\text{HFe}(\text{OCH}_2)^+$  (**2**), and their interconversion by  $\beta$ -hydrogen transfer via TS 1/2 (Scheme 1). Transition-metal alkoxide cations were first examined by Freiser and co-workers,<sup>12</sup> who have reported that the mass-spectrometric distinction between **1** and **2** is not straightforward because the potential interconversion of both isomers hampers a definitive structural assignment.<sup>13,14</sup> Furthermore, the electronic situation in open shell species such as **1** and **2** is quite different as compared to the closed-shell systems described by Versluis and Ziegler.<sup>5,7</sup> The focus of the present paper is to provide a detailed structural and energetic description of **1** and **2**, which may help to elucidate the common aspects and the differences of  $\beta$ -hydrogen transfer in 16- or 18-electron complexes versus the hitherto imperfectly rationalized open-shell species, such as  $\text{Fe}(\text{OCH}_3)^+$ . To this end, we performed combined mass spectrometric and computational studies on the  $[\text{Fe}, \text{C}, \text{H}_3, \text{O}]^+$  system which serves as a simple model to understand the  $\beta$ -hydrogen transfer in organometallic compounds. Experimentally, we find that independent generation of pure **1** and **2** is difficult, but a characterization of these species can be accomplished with little ambiguity.

## Experimental and Computational Details

The experiments use three completely different types of mass spectrometers. In brief, these experiments can be described as follows: (i) ion structures of  $[\text{Fe}, \text{C}, \text{H}_3, \text{O}]^+$  isomers were probed by high-energy collision-induced dissociation (CID) and related experiments in a sector field mass spectrometer (Sector-MS); (ii) the thermochemistry of **1** and **2** was assessed by threshold-CID and ion/molecule reactions at elevated kinetic energies using a guided ion beam (GIB) apparatus; and (iii) the bimolecular reactivity of **1** and/or **2** was examined using a Fourier transform ion cyclotron resonance (FTICR) mass spectrometer. Because the experimental setups have been described in detail in previous publications,<sup>15–18</sup> we limit ourselves here to the essential aspects.

(10) See, for example: (a) van Koppen, P. A. M.; Brodbelt-Lustig, J. F.; Bowers, M. T.; Dearden, D. V.; Beauchamp, J. L.; Fisher, E. R.; Armentrout, P. B. *J. Am. Chem. Soc.* **1990**, *112*, 5663. (b) Schröder, D.; Schwarz, H. *J. Am. Chem. Soc.* **1990**, *112*, 5947. (c) Schultz, R. H.; Armentrout, P. B. *J. Am. Chem. Soc.* **1991**, *113*, 729. (d) van Koppen, P. A. M.; Brodbelt-Lustig, J.; Bowers, M. T.; Dearden, D. V.; Beauchamp, J. L.; Fisher, E. R.; Armentrout, P. B. *J. Am. Chem. Soc.* **1991**, *113*, 2359. (e) Schröder, D.; Zummack, W.; Schwarz, H. *J. Am. Chem. Soc.* **1994**, *116*, 5857.

(11) (a) Czekay, G.; Drewello, T.; Schwarz, H. *J. Am. Chem. Soc.* **1989**, *111*, 4561. (b) Czekay, G.; Drewello, T.; Eller, K.; Zummack, W.; Schwarz, H. *Organometallics* **1989**, *8*, 2439.

(12) (a) Carlin, T. J.; Sallans, L.; Cassady, C. J.; Jacobson, D. B.; Freiser, B. S. *J. Am. Chem. Soc.* **1983**, *105*, 6320. (b) Cassady, C. J.; Freiser, B. S.; McElvany, S. W.; Allison, J. J. *J. Am. Chem. Soc.* **1984**, *106*, 6125. (c) Cassady, C. J.; Freiser, B. S. *J. Am. Chem. Soc.* **1985**, *107*, 1566.

(13) Halle, L. F.; Klein, F. S.; Beauchamp, J. L. *J. Am. Chem. Soc.* **1984**, *106*, 2543.

(14) Schröder, D.; Schwarz, H. *Angew. Chem., Int. Ed. Engl.* **1990**, *29*, 910.

(15) (a) Srinivas, R.; Sülzle, D.; Weiske, T.; Schwarz, H. *Int. J. Mass Spectrom. Ion Processes* **1991**, *107*, 368. (b) Srinivas, R.; Sülzle, D.; Koch, W.; DePuy, C. H.; Schwarz, H. *J. Am. Chem. Soc.* **1991**, *113*, 5970.

(16) Ervin, K. M.; Armentrout, P. B. *J. Chem. Phys.* **1985**, *83*, 166.

(17) Schultz, R. H.; Armentrout, P. B. *Int. J. Mass Spectrom. Ion Processes* **1991**, *107*, 29.

(18) (a) Eller, K.; Schwarz, H. *Int. J. Mass Spectrom. Ion Processes* **1989**, *93*, 243. (b) Eller, K.; Zummack, W.; Schwarz, H. *J. Am. Chem. Soc.* **1990**, *112*, 621.

**Sector-MS:**<sup>15</sup> A modified four-sector tandem mass-spectrometer of BEBE configuration (B stands for magnetic and E for electric sector) was used, in which MS-I is a VG ZAB-HF-2F and MS-II an AMD 604 double focusing mass spectrometer. Ions were generated by chemical ionization of ca. 1:1 mixtures of  $\text{Fe}(\text{CO})_5$  with appropriate precursor molecules (see below). The ions of interest, having 8 keV translational energy, were mass-selected by means of B(1)/E(1) at a mass resolution of  $m/\Delta m \approx 4000$ , and the unimolecular or collision-induced reactions (collision gas: helium at 80% transmission, T) occurring in the field-free region between E(1) and B(2) were recorded by scanning B(2). Neutralization–reionization (NR)<sup>19</sup> experiments were performed by colliding B(1)/E(1) mass-selected ions with xenon (80% T), deflecting the remaining ions by applying a potential of 1 kV, reionizing the fast neutrals by collision with oxygen (80% T), and detecting the so-formed cations by scanning B(2). Spectra were recorded with the AMD Intectra data system; typically, 10–20 spectra were accumulated.

**GIB:** The guided ion beam apparatus used in this study and our data reduction procedures have been described previously.<sup>16,17</sup>  $\text{FeL}^+$  ( $\text{L} = \text{OCD}_3$  and  $\text{CH}_2\text{O}$ ) ions were produced in a meter-long flow tube ion source operating at a pressure of 0.4–0.7 Torr with helium flow rates of 4000–9000 standard  $\text{cm}^3/\text{min}$ .  $\text{Fe}^+$  was produced by argon ion sputtering of an iron cathode in a flow of 5–10% argon in helium. The desired complexes were formed by introducing reagents into the flow tube in a flow of helium ca. 10 cm downstream from the dc discharge.  $\text{Fe}(\text{OCD}_3)^+$  was formed by reaction of  $\text{Fe}^+$  with  $[\text{D}_3]$ -nitromethane<sup>12</sup> and  $\text{Fe}(\text{OCH}_2)^+$  by three-body association reactions of  $\text{Fe}^+$  and formaldehyde, respectively. The ions undergo  $\sim 10^5$  collisions with the buffer gas before exiting the flow tube, and therefore are expected to have equilibrated to a temperature of 300 K with respect to all internal states. Previous work on a number of systems<sup>20</sup> is consistent with the production of thermalized ions under similar conditions.

The ions were extracted from the source, accelerated, and focused into a magnetic sector momentum analyzer for mass analysis. Mass-selected ions were decelerated to a desired kinetic energy and focused into an octopole ion trap.<sup>16</sup> This device guides the ions through a static gas cell containing sufficiently low pressure ( $\sim 0.05$ – $0.2$  mTorr) of  $\text{D}_2$  or Xe such that multiple collisions are improbable. After exiting the gas cell, product and unreacted beam ions drift to the end of the octopole where they are directed into a quadrupole mass filter for mass analysis and then detected by using a Daly-type detector and pulse-counting electronics. Conversion of the raw ion intensities into reaction cross-sections and the calibration of the absolute energy scale were treated as described previously.<sup>16</sup> The accuracy of our absolute cross sections for room temperature data is estimated to be  $\pm 20\%$ . The beams were found to have Gaussian kinetic energy distributions with a fwhm of  $\sim 0.34$  eV in the laboratory frame with uncertainties of  $\pm 0.05$  eV in the absolute energy scale. It was verified that all product cross sections reported were results of single ion/molecule collisions by examining the pressure dependence of the product intensities.

Quantitative analysis of the energy dependence of these cross sections was achieved using methods that are outlined elsewhere.<sup>21</sup> Determination of the reaction thresholds involves explicit consideration of the distributions of vibrational, rotational, and translational energies such that the values obtained correspond to 0 K bond dissociation energies (BDEs). The vibrational frequencies used in these determinations were taken from the calculations described below after scaling to 90%.

**FTICR:**<sup>18</sup> These experiments were performed with a *Spectrospin CMS 47X* FTICR mass spectrometer.  $\text{Fe}^+$  was formed by laser

(19) (a) For recent reviews, see: Goldberg, N.; Schwarz, H. *Acc. Chem. Res.* **1994**, *27*, 347. (b) Zagorevskii, D. V.; Holmes, J. L. *Mass Spectrom. Rev.* **1994**, *13*, 133.

(20) (a) Khan, F. A.; Clemmer, D. E.; Schultz, R. H.; Armentrout, P. B. *J. Chem. Phys.* **1993**, *97*, 7978. (b) Dalleska, N. F.; Honma, K.; Armentrout, P. B. *J. Am. Chem. Soc.* **1993**, *115*, 12125. (c) Dalleska, N. F.; Honma, K.; Sunderlin, L. S.; Armentrout, P. B. *J. Am. Chem. Soc.* **1994**, *116*, 3519. (d) Tjelta, B. L.; Armentrout, P. B. *J. Am. Chem. Soc.* **1995**, *117*, 5531.

(21) (a) Armentrout, P. B. In *Advances in Gas Phase Ion Chemistry*; Adams, N. G., Babcock, L. M., Eds.; JAI: Greenwich, 1992; Vol. 1, pp 83–119. (b) Schultz, R. H.; Crellin, K. C.; Armentrout, P. B. *J. Am. Chem. Soc.* **1991**, *113*, 8590.

desorption/laser ionization<sup>22</sup> of an iron rod in the external ion source and transferred to the analyzer cell which is located within a superconducting magnet (maximum field strength 7.05 T). Subsequently,  $^{56}\text{Fe}^+$  was mass-selected, thermalized by pulsed-in argon (ca. 500 collisions), and reacted with pulsed-in precursors, e.g.  $\text{CD}_3\text{NO}_2$  to yield  $[\text{Fe}, \text{C}, \text{D}_3, \text{O}]^+$  or  $\text{N}_2\text{O}/\text{CH}_4$  to yield  $\text{FeOH}^+$ . Other reagent gases were introduced into the FTICR cell via leak valves at typical pressures of  $(4\text{--}20) \times 10^{-9}$  mbar. CID was brought about by kinetic excitation of the ions of interest by irradiation of the appropriate frequency and subsequent collision of the excited ions with argon  $(2\text{--}4) \times 10^{-8}$  mbar).<sup>23</sup> The collision energy was between 3 and 5 eV at approximate single-collision conditions. The determination of the absolute collision energy in FTICR experiments is not straightforward, and we refrain from an exact quantification. However, this uncertainty does not matter for the comparative purposes for which CID is applied here. All data were accumulated and on-line processed using an ASPECT 3000 mini-computer.

**Calculations:** For the computational study of **1**, **2**, and TS **1/2**, a DFT approach was applied in which the Becke3LYP functional<sup>24</sup> was combined with Wachters<sup>25</sup> (16s10p6d)[8s5p3d] and Dunning/Huzinaga<sup>26</sup> D95\*\* basis sets. All calculations were performed with the GAUSS-92/DFT program package.<sup>27</sup> The energetic accuracy of this approach<sup>28</sup> for transition-metal compounds has previously been examined for the  $[\text{Fe}, \text{C}_2, \text{H}_6]^+$  system and is on the order of  $0 < \Delta\text{BDE} < 20$  kcal/mol for bond-dissociation energies and  $\pm 5$  kcal/mol for the relative energies of isomers.<sup>29</sup> An indication of the accuracy of the calculations for different spin states is obtained by examining the energetics of the  $^4\text{F}$  and  $^6\text{D}$  states of  $\text{Fe}^+$ . At the level of theory employed, the  $\text{Fe}^+(^4\text{F})$  state is computed to be 2 kcal/mol more stable than the  $\text{Fe}^+(^6\text{D})$  state, while the experimental splitting is 5.8 kcal/mol in favor of the sextet state. This trend should persist in the molecular calculations; however, it is not clear how this error translates quantitatively. Corrections for zero-point energy have been taken into account, but the basis set effects have not been addressed. Therefore, the energetics discussed here should only be taken as a guideline for the interpretation of the experimental findings. Unfortunately, a number of species considered in the theoretical treatment bear small imaginary frequencies in the analytical calculations of the eigenvalues. A more detailed analysis revealed that these can be attributed to the numerical noise and the non-rotational invariance of the numerical grid used, as well as to problems associated with symmetry breaking in the single-determinant approach.<sup>30</sup> These effects became evident from the fact that bending by small amounts (e.g.  $1^\circ$ ) or rotations of the molecule in the standard orientation resulted in quite different (and sometimes imaginary) frequencies. Therefore, we performed the optimizations in  $C_1$  symmetry.

## Results and Discussion

This section is organized such that we first discuss conceivable structures of  $[\text{Fe}, \text{C}, \text{H}_3, \text{O}]^+$  isomers and try to distinguish them by means of high-energy collision experiments in the sector-MS. Next, we address the experimentally determined

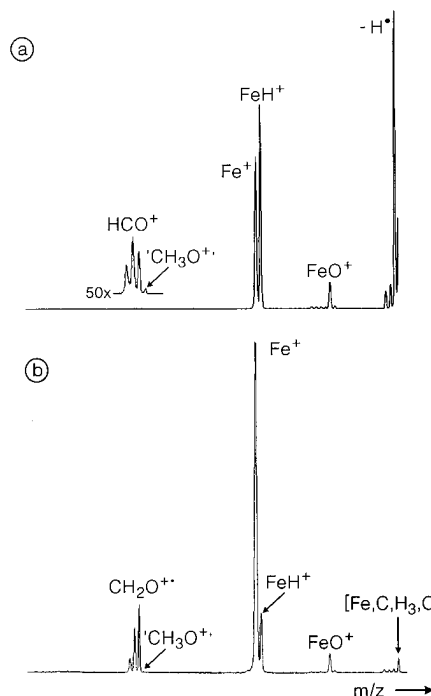
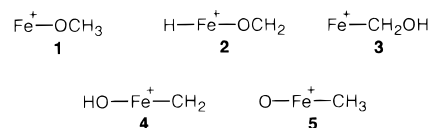


**Figure 1.** (a) CID mass spectrum (He, 80% T) and (b) NR mass spectrum (Xe/O<sub>2</sub>, each 80% T) of  $[\text{Fe}, \text{C}, \text{H}_3, \text{O}]^+$  generated by chemical ionization of  $\text{Fe}(\text{CO})_5$  and nitromethane.

## Scheme 2



thermodynamics of the crucial isomers **1** and **2** using the GIB methodology. Then the interconversion  $\mathbf{1} \rightleftharpoons \mathbf{2}$  is discussed in detail together with a presentation of the computational results for the quintet and triplet potential-energy hypersurfaces. This is followed by an analysis of the bimolecular reactivity of **1**, and finally, the role of ligand effects and their implications for condensed-phase chemistry of metal alkoxide isomerization are discussed.

**Ion Structures.** From a chemical point of view five different connectivities are conceivable for  $[\text{Fe}, \text{C}, \text{H}_3, \text{O}]^+$  cations (Scheme 2). In order to probe whether these isomers are experimentally accessible and to which extent interconversion processes take place, we attempted to generate  $[\text{Fe}, \text{C}, \text{H}_3, \text{O}]^+$  by means of chemical ionization and characterize them using high-energy CID in the sector instrument.<sup>31</sup> Formally, cationic iron(II) methoxide (**1**) can be generated from  $\text{Fe}^+$  and a variety of precursors  $\text{CH}_3\text{O}-\text{X}$  which contain a suitable leaving group X, e.g. X = Cl, NO, and OR. **1** is also accessible in the reaction of  $\text{Fe}^+$  with nitromethane.<sup>12,14,32,33</sup> The CID mass spectrum of  $[\text{Fe}, \text{C}, \text{H}_3, \text{O}]^+$  ion formed in the latter reaction (Figure 1a) shows an abundant loss of atomic hydrogen. This process would be expected to be quite facile for structures **1**–**3**, but not for **4** and **5**, since this would involve even higher formal oxidation states of iron than those already present in **4** and **5**. The two other prominent fragments, i.e.  $\text{FeH}^+$  and  $\text{Fe}^+$ , correspond to losses of neutral formaldehyde and a methoxy (or hydroxymethyl)

- (22) Freiser, B. S. *Talanta* **1985**, 32, 687.  
 (23) (a) Burnier, R. C.; Cody, R. B.; Freiser, B. S. *J. Am. Chem. Soc.* **1982**, 104, 7436. (b) Freiser, B. S.; Cody, R. B. *Int. J. Mass Spectrom. Ion Phys.* **1982**, 41, 199.  
 (24) Becke, A. D. *J. Chem. Phys.* **1993**, 98, 1372.  
 (25) (a) Wachters, A. J. H. *J. Chem. Phys.* **1970**, 52, 1033. (b) Hay, P. J. *J. Chem. Phys.* **1977**, 66, 4377.  
 (26) Dunning, T. H.; Hay, P. J. In *Modern Theoretical Chemistry*; Schaefer, H. F., Ed.; Plenum Press: New York, 1977; Vol. II.  
 (27) GAUSSIAN 92/DFT, Revision F.2, Frisch, M. J.; Trucks, G. W.; Schlegel, H. B.; Gill, P. M. W.; Johnson, B. G.; Wong, M. W.; Foresman, J. B.; Robb, M. A.; Head-Gordon, M.; Replogle, E. S.; Gomperts, R.; Andres, J. L.; Raghavachari, K.; Binkley, J. S.; Gonzalez, C.; Martin, R. L.; Fox, D. J.; Defrees, D. J.; Baker, J.; Stewart, J. J. P.; Pople, J. A.; GAUSSIAN Inc.: Pittsburgh, PA, 1993.  
 (28) For a detailed discussion of the theoretical aspects of this approach, see: (a) Holthausen, M. C.; Heinemann, C.; Cornehl, H. H.; Koch, W.; Schwarz, H. *J. Chem. Phys.* **1995**, 102, 4931. (b) Also see: Holthausen, M. C.; Mohr, M.; Koch, W. *Chem. Phys. Lett.* **1995**, 240, 245.  
 (29) Holthausen, M. C.; Fiedler, A.; Schwarz, H.; Koch, W. *Angew. Chem.* **1995**, 34, 2282.  
 (30) Morokuma, K.; Ahlrichs, R. Personal communications.

- (31) For a related approach to study  $[\text{Fe}, \text{C}, \text{H}_4, \text{O}]^+$  isomers, see: Schröder, D.; Fiedler, A.; Hrušák, J.; Schwarz, H. *J. Am. Chem. Soc.* **1992**, 114, 1215.  
 (32) Schröder, D. Ph.D. Thesis, Technische Universität Berlin D83, 1993.  
 (33) (a) Schalley, C. A.; Wesendrup, R.; Schröder, D.; Weiske, T.; Schwarz, H. *J. Am. Chem. Soc.* **1995**, 117, 7711. (b) Wesendrup, R.; Schalley, C. A.; Schröder, D.; Schwarz, H. *Chem. Eur. J.* **1995**, 1, 608.

**Table 1.** Heats of Formation ( $\Delta_f H$  in kcal/mol) of Dissociation Products of  $[\text{Fe}, \text{C}, \text{H}_3, \text{O}]^+$ 

species	$\Delta_f H^a$	species	$\Delta_f H^a$
$\text{Fe}(\text{OCH}_2)^+ + \text{H}^\bullet$	$274.5 \pm 1.6^b$	$\text{FeC}^+ + \text{H}_2\text{O} + \text{H}^\bullet$	$353.1 \pm 5.0$
$\text{FeOH}^+ + \text{CH}_2$	$300.9 \pm 4.1^c$	$\text{FeH}^+ + \text{CH}_2\text{O}$	$257.9 \pm 1.4$
$\text{FeO}^+ + \text{CH}_3^\bullet$	$294.9 \pm 1.2$	$\text{Fe}^+ + \text{CH}_2\text{OH}$	$277.0 \pm 0.3$
$\text{FeCH}_3^+ + \text{O}$	$320.2 \pm 1.1$	$\text{Fe}^+ + \text{CH}_3\text{O}^\bullet$	$285.5 \pm 0.9$
$\text{FeCH}_2^+ + \text{HO}^\bullet$	$301.6 \pm 0.9$	$\text{CH}_2\text{OH}^+ + \text{Fe}$	$267.3 \pm 2.6$
$\text{FeCH}^+ + \text{H}_2\text{O}$	$265.3 \pm 5.0$	$\text{CH}_2\text{O}^+ + \text{FeH}$	$340.9 \pm 0.9$

<sup>a</sup> Except as noted, all data refer to 298 K in the stationary electron convention and were taken from ref 35 for most of the organometallics and from ref 34 for the organic fragments. <sup>b</sup>  $\text{BDE}(\text{Fe}^+-\text{OCH}_2) = 33 \pm 1.6$  kcal/mol was taken from ref 42. <sup>c</sup>  $\text{BDE}(\text{Fe}^+-\text{OH})$  was taken as  $83 \pm 4$  kcal/mol. This is the average of the data reported in refs 34 and 35.

radical, respectively. Because these reactions imply an intact C–O bond in  $[\text{Fe}, \text{C}, \text{H}_3, \text{O}]^+$ , they also point to structures **1–3**. However, CID of structure **3** is expected to yield significant amounts of hydroxymethyl cation,  $\text{CH}_2\text{OH}^+$ , concomitant with loss of neutral Fe (Table 1), because the ionization energy of  $\text{CH}_2\text{OH}$  (7.56 eV) is lower than that of atomic Fe (7.90 eV).<sup>34,35</sup> Experimentally,  $\text{CH}_2\text{OH}^+$  is barely observed (<1%) in the CID mass spectrum. In addition, the intense signal for the  $\text{FeO}^+$  fragment suggests the presence of an Fe–O bond together with an intact methyl group which is in line with structure **1**. Despite these features no unambiguous distinction between **1** and **2** can be made on the basis of the experimental findings. Unfortunately, all our attempts to generate isomeric ions from different precursor mixtures<sup>36</sup> resulted in fragmentation patterns very similar to that shown in Figure 1a for the  $[\text{Fe}, \text{C}, \text{H}_3, \text{O}]^+$  ions generated from  $\text{Fe}(\text{CO})_5$  and nitromethane.

Often, NR experiments<sup>19</sup> have served as an alternative to circumvent this dilemma in structural assignment, because isomerization processes, which may be facile in cations, are hampered in the corresponding neutral species. This holds particularly true for hydrogen migrations, as between **1** and **2**.<sup>37</sup> The NR spectrum of  $[\text{Fe}, \text{C}, \text{H}_3, \text{O}]^+$  generated from nitromethane and  $\text{Fe}(\text{CO})_5$  (Figure 1b) is dominated by the  $\text{Fe}^+$  signal which, however, is not structure indicative. In addition, a signal for the reionized neutral  $[\text{Fe}, \text{C}, \text{H}_3, \text{O}]$  is observed. With respect to the ion structure, the  $\text{FeO}^+$  fragment is in keeping with structure **1**, while the  $\text{FeH}^+$  signal suggests the presence of **2**. The absence of a signal for  $\text{CH}_3\text{O}^+$  does not rule out **1**, because Fe has a lower ionization energy than  $\text{CH}_3\text{O}$ <sup>34</sup> and even an intact methoxy group is unlikely to generate  $\text{CH}_3\text{O}^+$  due to the intrinsic instability of alkoxide cations.<sup>38</sup> Vice versa, the weak signal for  $[\text{C}, \text{H}_3, \text{O}]^+$  excludes **3**, while the relative intensities of the other  $[\text{C}, \text{H}_n, \text{O}]^+$  ions ( $n = 0–2$ ) again indicate the presence of an intact C–O bond. Thus, we have to conclude that we can rule out structures **3–5**, but a definitive distinction between **1** and **2** cannot be provided by the otherwise powerful techniques

(34) (a) Relevant thermochemical data were taken from: Lias, S. G.; Bartmess, J. E.; Liebman, J. F.; Holmes, J. L.; Levin, R. D.; Mallard, W. G. *Gas Phase Ion and Neutral Thermochemistry*. *J. Phys. Chem. Ref. Data, Suppl. 1* **1988**, 17. (b) An accurate value of  $\text{IE}(\text{Fe}) = 7.90$  eV was taken from: Sugar, J.; Corliss, C. J. *Phys. Chem. Ref. Data Suppl. 2* **1985**, 14.

(35) Additional thermochemical information on organometallic ions was taken from: Armentrout, P. B.; Kickel, B. L. In *Organometallic Ion Chemistry*; Freiser, B. S., Ed.; Kluwer: Dordrecht, 1995; pp 1–45.

(36) Analogous to ref 31, the following mixtures were subjected to chemical ionization in the hope of obtaining  $[\text{Fe}, \text{C}, \text{H}_3, \text{O}]^+$  isomers:  $\text{Fe}(\text{CO})_5$  and  $\text{X}-\text{CH}_2\text{OH}$  to yield **3** ( $\text{X} = \text{H}, \text{CH}_3, \text{Me}_3\text{Si}$ ),  $\text{Fe}(\text{CO})_5$ ,  $\text{N}_2\text{O}$ ,  $\text{CH}_4$ , and  $c\text{-C}_3\text{H}_6$  to give **4**, and  $\text{Fe}(\text{CO})_5$ ,  $\text{N}_2\text{O}$ , and  $\text{CH}_3\text{I}$  to form eventually **5**. However, within experimental error, all CID spectra were indistinguishable from that shown in Figure 1a. Consequently, either **3–5** were not formed at all or they rapidly isomerize to **1** and/or **2** under CI conditions.

(37) Schröder, D.; Sülzle, D.; Hrušák, J.; Bohme, D. K.; Schwarz, H. *Int. J. Mass Spectrom. Ion Processes* **1991**, 110, 145.

(38) Burgers, P. C.; Holmes, J. L. *Org. Mass Spectrom.* **1984**, 19, 452.

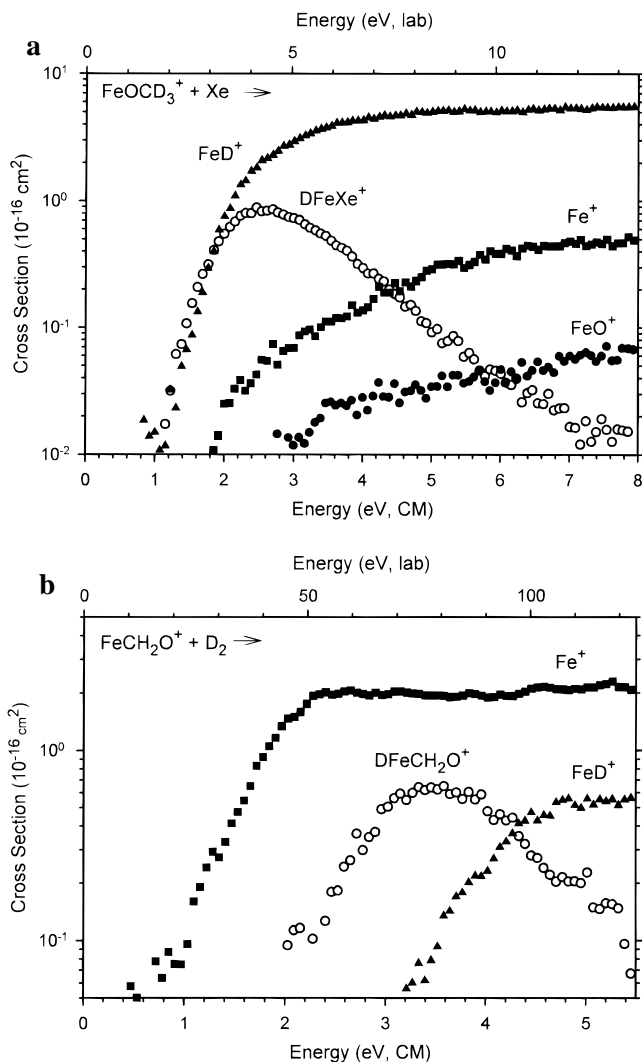
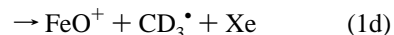
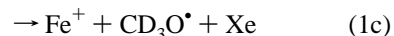
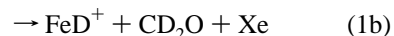


**Figure 2.** (a) Cross sections for the reaction of  $[\text{Fe}, \text{C}, \text{D}_3, \text{O}]^+$  with xenon as a function of relative kinetic energy (lower x-axis) and laboratory energies (upper x-axis). (b) Cross sections for the reaction of  $\text{Fe}(\text{CH}_2\text{O})^+$  with  $\text{D}_2$  as a function of relative kinetic energy (lower x-axis) and laboratory energies (upper x-axis).

applied here (see below). In fact, these findings highlight the ease of interconversion processes in organometallic gas-phase ion chemistry that may lead to the formation of isomeric mixtures and render the characterization of different isomers often difficult.

**Energetics.** The thermochemistry of **1** and **2** was investigated in threshold-CID experiments using the GIB methodology by colliding either  $\text{FeOCD}_3^+$  with Xe or  $\text{Fe}(\text{OCH}_2)^+$  with  $\text{D}_2$  under single-collision conditions. In the following discussion, we assume that the thermochemistry for deuterium containing compounds is equal to that of hydrogen-containing compounds within any experimental errors.

In the first experiment, four major reaction channels were observed (Figure 2a):



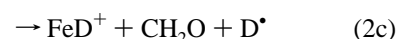
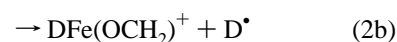
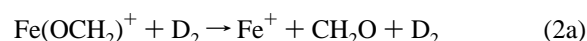
Except for reaction 1a, these products were also observed in

the high-energy CID (Figure 1a). Failure to observe  $[\text{C}_n\text{D}_n\text{O}]^+$  ( $n = 0-3$ ) is consistent with such products being much higher energy species than the ionic products of reaction 1. Failure to observe the D-atom loss product,  $\text{Fe}(\text{OCD}_2)^+$ , is in part due to the need to operate the GIB apparatus at low mass resolution in order to measure accurate cross sections. In addition, comparison of CID experiments in sector and FTICR MS reveals that D-atom loss is strongly favored in high-energy collisions, while it is much less abundant in low-energy CID in which fragmentation to  $\text{FeD}^+$  and  $\text{Fe}^+$  predominate.<sup>12a,32</sup> Hence, observation of  $\text{Fe}(\text{OCD}_2)^+$ , only two mass units below the much more intense reactant ion beam, is particularly difficult in the GIB experiment.

At the lowest energies, we observe the formation of  $\text{DFeXe}^+$ , and at slightly higher energies this product loses the rare gas atom and we observe the formation of  $\text{FeD}^+$ . Threshold analyses of the  $\text{DFeXe}^+$  and  $\text{FeD}^+$  cross sections yield 0 K energy thresholds of  $1.46 \pm 0.03$  and  $1.83 \pm 0.05$  eV, respectively. Because reactions 1a and 1b differ only by the rare gas atom complexed to the  $\text{FeD}^+$  fragment, the difference in these thresholds provides the bond dissociation energy (BDE),  $D_0(\text{DFe}^+-\text{Xe}) = 8.5 \pm 1.3$  kcal/mol. This is essentially identical to the BDE of Xe to the bare metal ion,  $D_0(\text{Fe}^+-\text{Xe}) = 9.0 \pm 1.4$  kcal/mol.<sup>21b,39</sup> This is reasonable as both  $\text{Fe}^+$  ( $^6\text{D}$ ,  $4s^13d^6$ ) and  $\text{FeH}^+$  ( $^5\Delta$ ,  $\sigma^23d^6$ ) have occupied 4s-like orbitals. The threshold for reaction 1b can also be combined with the heats of formation ( $\Delta_f H$ )<sup>34</sup> of  $\text{Fe}^+$ ,  $\text{H}^+$ ,  $\text{CH}_2\text{O}$ , and  $\text{CH}_3\text{O}^+$  and  $D_0(\text{Fe}^+-\text{H}) = 48.9 \pm 1.4$  kcal/mol<sup>35</sup> to yield a heat of formation for the  $[\text{Fe}, \text{C}, \text{H}_3, \text{O}]^+$  ion of  $216.6 \pm 2.0$  kcal/mol. We attribute this heat of formation to isomer **1**, for reasons which will become evident shortly. This heat of formation corresponds to a value of  $69.0 \pm 2.0$  kcal/mol for  $D_0(\text{Fe}^+-\text{OCH}_3)$ . This  $\text{Fe}^+-\text{OCH}_3$  bond energy can be compared to  $D_0(\text{Fe}^+-\text{OH}) = 83 \pm 4$  kcal/mol.<sup>34,35</sup> The difference is comparable to that observed between  $D_0(\text{H}-\text{OH}) = 118.1 \pm 0.1$  kcal/mol<sup>40</sup> and  $D_0(\text{H}-\text{OCH}_3) = 103 \pm 1$  kcal/mol,<sup>41</sup> and therefore reflects the stability of the methoxy vs hydroxy radicals. This favorable comparison supports the assignment of isomer **1**.

The cross sections for  $\text{Fe}^+$  and  $\text{FeO}^+$  are difficult to analyze because their shapes indicate that two distinct processes are contributing to each ionic product. The predominant features at higher energies in both cross sections are consistent with thermochemistry derived from reaction 1b, namely thresholds of  $2.97 \pm 0.08$  and  $3.43 \pm 0.10$  eV for reactions 1c and 1d, respectively. A more detailed analysis of the data indicates that the low-energy features are consistent with formation of **2** and its thermochemistry derived in the second GIB experiment (see below). This suggests that isomers **1** and **2** are present in the  $[\text{Fe}, \text{C}, \text{D}_3, \text{O}]^+$  ions produced by reaction of  $\text{Fe}^+$  with nitromethane in the flow-tube source, with the latter ion as a minor component. We cannot, however, exclude interferences from other (unknown) impurities in the  $[\text{Fe}, \text{C}, \text{D}_3, \text{O}]^+$  beam.

Results for the interaction of  $\text{D}_2$  with  $\text{Fe}(\text{OCH}_2)^+$  are shown in Figure 2b. We observe three products formed in reactions 2a-2c.



The major product is  $\text{Fe}^+$ , formed in the simple CID reaction 2a which has a thermodynamic threshold of  $1.43 \pm 0.07$  eV (Table 1) taken from previous data from our laboratories for  $\text{BDE}(\text{Fe}^+-\text{OCH}_2)$ .<sup>42</sup> As the energy is increased, the two channels involving  $\text{D}_2$  activation,<sup>20d</sup> reactions 2b and 2c, are observed. (Observation of  $\text{DFe}(\text{OCH}_2)^+$ , only two mass units above the much more intense reactant ion beam, is possible in this experiment because it lies to the high mass side of the reactant ion, where the mass overlap is considerably less than to the low mass side.) It can be seen that these channels are coupled because the cross section for the  $\text{DFe}(\text{OCH}_2)^+$  product begins to decline at an energy where the formaldehyde ligand can fall off, the threshold for formation of  $\text{FeD}^+$ . This product has a thermodynamic threshold of  $3.88 \pm 0.12$  eV (Table 1). The cross sections for reactions 2a and 2c can be modeled accurately using the thermochemical data in Table 1. For process 2b, our analysis yields a threshold of  $2.65 \pm 0.07$  eV. Following the same type of thermochemical arguments as outlined above, we derive  $\Delta_f H = 231.4 \pm 3.0$  kcal/mol for the  $[\text{Fe}, \text{C}, \text{H}_3, \text{O}]^+$  isomer formed in reaction 2b. This value differs from that derived from reaction 1b by  $15 \pm 4$  kcal/mol, much larger than the error limits of the experiments. Therefore, we conclude that the threshold of reaction 2b corresponds to the formation of **2** via D-D bond activation by the metal without active participation of the formaldehyde ligand. The fact that two different heats of formation can be determined in this type of experiment implies that the barrier for the unimolecular interconversion  $\mathbf{1} \rightleftharpoons \mathbf{2}$  is significant (see below), as otherwise reaction 2b would exhibit a thermochemical threshold characteristic of **1**, i.e. ca. 2.05 eV. Furthermore, if reaction 2b formed **1**, i.e.  $\text{Fe}(\text{OCH}_2\text{D})^+$ , then  $\text{FeH}^+$  should have been generated in the subsequent dissociation. Despite a careful search, no  $\text{FeH}^+$  product was observed, which lends further support to the conclusion that a considerable barrier separates **1** and **2**. Unfortunately, the experiments do not allow a quantitative estimate of the energy of this barrier.

An alternative method to estimate the thermochemistry of **1** is provided by the observation of ion-molecule reactions 3:



Under the conditions of FTICR mass spectrometry, we observe reaction 3 for  $\text{X} = \text{OH}$  and  $\text{F}$ , but not for  $\text{X} = \text{Cl}$ ,<sup>43</sup> which provides an upper limit of  $\Delta_f H^\circ[\text{Fe}, \text{C}, \text{H}_3, \text{O}]^+ = 217$  kcal/mol. On the basis of the thermochemistry determined above, this figure is in line with the exclusive formation of  $\text{Fe}(\text{OCD}_3)^+$  in the reaction of  $\text{FeX}^+$  ( $\text{X} = \text{F}, \text{OH}$ ) with  $\text{CD}_3\text{OH}$  and provides further evidence against the generation of isomers **2** and **3**. Interestingly, although the strength of the C-H bond in methanol is significantly weaker than that of the O-H bond (94 versus 104 kcal/mol), the reaction of  $\text{FeX}^+$  with  $\text{CD}_3\text{OH}$  results in only O-H bond activation,<sup>44</sup> and no C-H bond

(39) Schultz, R. H.; Armentrout, P. B. *J. Phys. Chem.* **1993**, *97*, 596.

(40) Calculated from heats of formation given by: Gurvich, L. V.; Veyts, I. V.; Alcock, C. B. *Thermodynamic Properties of Individual Substances*, 4th ed.; Hemisphere: New York, 1989; Vol. 1, Part 2. Chase, M. W., Jr.; Davies, C. A.; Downey, J. R., Jr.; Frurip, D. J.; McDonald, R. A.; Syverud, A. N. *J. Phys. Chem. Ref. Data* **1985**, *14*, Suppl. No. 1 (JANAF Tables).

(41)  $\Delta_f H^\circ(\text{H})$  taken from the JANAF Tables, see ref 40.  $\Delta_f H^\circ_{298}(\text{OCH}_3)$  taken from: Berkowitz, J.; Ellison, G. B.; Gutman, D. *J. Phys. Chem.* **1994**, *98*, 2744.  $\Delta_f H^\circ_{298}$  values are converted to  $\Delta_f H^\circ_0$  by using values in: Wagman, D. D.; Evans, W. H.; Parker, V. B.; Schumm, R. H.; Halow, I.; Bailey, S. M.; Churney, K. L.; Nuttall, R. L. *J. Phys. Chem. Ref. Data* **1982**, *11*, 1.

(42) For previous values for  $\text{BDE}(\text{Fe}^+-\text{OCH}_2) = 33.4$  and  $33.0$  kcal/mol, respectively, see: (a) Schröder, D.; Schwarz, H. *J. Organomet. Chem.* **1995**, *504*, 123. (b) Tjelta, B. L.; Armentrout, P. B. Unpublished results.

(43)  $\text{BDE}(\text{Fe}^+-\text{Cl}) = 84$  kcal/mol; see: (a) Fisher, E. R.; Schultz, R. H.; Armentrout, P. B. *J. Phys. Chem.* **1989**, *93*, 7382. (b) Schröder, D.; Hrušák, J.; Schwarz, H. *Ber. Bunsenges. Phys. Chem.* **1993**, *97*, 1086.

(44) Blum, O.; Stöckigt, D.; Schröder, D.; Schwarz, H. *Angew. Chem., Int. Ed. Engl.* **1992**, *31*, 603.

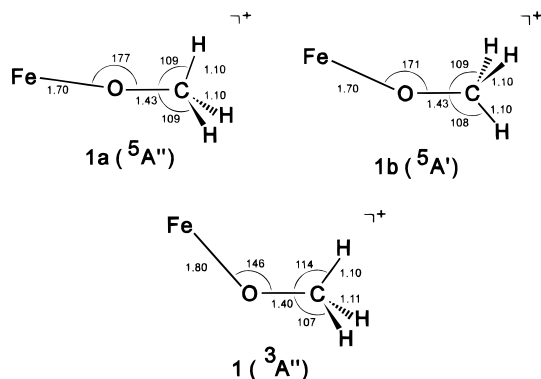


**Figure 3.** Structures of **1a** ( $^5A''$ ), **1b** ( $^5A'$ ), and **1** ( $^3A''$ ); bond lengths in Å and bond angles in degrees.

activation. Hence formation of **3** is either endothermic or hindered by a considerable kinetic barrier.

**Computations.** Although the computations are not intended to reproduce the experimental thermochemistry quantitatively, they do provide a useful guideline to qualitatively verify the experimental interpretation. The iron methoxide cation **1** is formally generated by spin pairing ground state atomic  $\text{Fe}^+$  ( $^6D$ ) with doublet  $\text{CH}_3\text{O}^\bullet$  ( $^2E$ ). Hence, **1** is expected to have a quintet ground state. In  $C_s$  symmetry, two conformations are conceivable for the bent molecule, i.e. an eclipsed (**1a**) and a staggered (**1b**) conformer (Figure 3). The eclipsed conformation **1a** should be favored if  $\beta$ -agostic stabilization between the electron-deficient iron and the doubly occupied  $\sigma$ -orbital of the eclipsed C-H bond is operative. Vice versa, the staggered conformer **1b** should be more stable if Pauli repulsion between the Fe-O and the C-H bonds dominates. For these two quintet states, the calculations reveal that the classical conformer **1b** ( $^5A'$ ) is slightly less stable ( $\Delta E = 0.5$  kcal/mol) than **1a** ( $^5A''$ ); however, this difference is on the order of the numerical accuracy of the calculations.<sup>45</sup> Furthermore, the quintet states of **1a** and **1b** are almost linear ( $\alpha_{\text{Fe-O-C}} = 177^\circ$  and  $171^\circ$ , respectively)<sup>46</sup> and show nearly undisturbed methoxy units,<sup>47</sup> such that we conclude that agostic stabilization is negligible. Ground state **1** ( $^5A''$ ) is calculated to have a BDE( $\text{Fe}^+ - \text{OCH}_3$ ) of 85 kcal/mol, 79 kcal/mol after zero-point vibrational energies (ZPVEs) are considered. Both values are substantially larger than the experimental figure of  $69 \pm 2$  kcal/mol. This discrepancy can be ascribed to the known systematic underestimation of exchange-energy loss through bond formation in the DFT approach.<sup>48</sup> The energetically lowest-lying triplet state **1** ( $^3A''$ ) is calculated to lie 31 kcal/mol higher in energy than **1a** ( $^5A''$ ), a value unchanged by ZPVE effects. This state has a bent ( $\alpha_{\text{Fe-O-C}} = 146^\circ$ ) minimum structure that prefers the eclipsed form with a significantly elongated Fe-O bond. Although the decreased FeOC and OCH bond angles of **1** ( $^3A''$ ) point to a  $\beta$ -agostic interaction, the differences of the C-H bond lengths are marginal when comparing **1** ( $^3A''$ ) and free  $\text{OCH}_3$ . Obviously, in this particular structure of **1** ( $^3A''$ ), there is a subtle balance between the repulsive interactions between filled orbitals and the weak agostic attraction of a  $\beta$ -H atom and the iron center.

**2** can be described in terms of a complex of the  $\text{FeH}^+$  cation interacting with the formaldehyde dipole. According to several

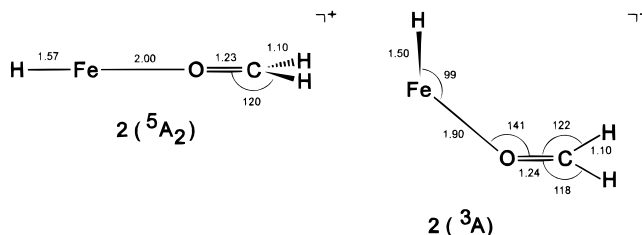


**Figure 4.** Structures of **2** ( $^5A_2$ ) and **2** ( $^3A$ ).

previous ab initio calculations,<sup>49</sup>  $\text{FeH}^+$  exhibits a  $^5\Delta$  ground state, such that complexation of formaldehyde is expected to give rise to a quintet ground state for **2**. A triplet (low-spin) ground state would only be favored in the case of a much stronger ligand field than that generated by a single formaldehyde molecule. These qualitative arguments are confirmed by the calculations. The quintet state **2** ( $^5A_2$ ) is 21 kcal/mol more stable than the triplet state **2** ( $^3A$ ), a value unchanged by ZPVE corrections. The BDE of  $\text{HFe}^+ - \text{OCH}_2$  is computed as 47 kcal/mol, again larger than the experimental value of  $28 \pm 3$  kcal/mol. The computational overestimate is similar to that for **1** ( $^5A''$ ). The stability difference between **1** ( $^5A''$ ) and **2** ( $^5A_2$ ) is calculated to be 9 kcal/mol (6 kcal/mol after ZPVE corrections) as compared to the experimental figure of  $15 \pm 4$  kcal/mol. This is reasonable agreement considering the limitations of our computational approach and the expected uncertainty for the computed relative energetics of  $\pm 5$  kcal/mol.<sup>28</sup> The optimized geometry of **2** ( $^5A_2$ ) exhibits  $C_{2v}$  symmetry with a short (covalent) Fe-H bond (1.57 Å) and a longer Fe-O distance of 2.00 Å (Figure 4), as expected for a simple complexation of  $\text{CH}_2\text{O}$ . Likewise, the formaldehyde subunit shows a geometry that is hardly perturbed compared to the isolated molecule with similar bond lengths and angles.<sup>50</sup> Interestingly, the energy of **2** is quite insensitive to the bending of the H-Fe-O and the Fe-O-C angles, and hence, the bending forces and the frequencies for these modes are very small.<sup>51</sup> The energetically lowest-lying triplet state **2** ( $^3A$ ) deviates from linearity of the H-Fe-O-C unit, and  $r_{\text{Fe-O}}$  is shortened to 1.90 Å which indicates a contribution of a resonance structure in which neutral iron is bound to an oxonium center. However, the bending forces are quite small as reflected by a difference of only 5 kcal/mol between the vertical excitation energy of **2** ( $^5A_2$ ) to the triplet surface and the energy of the geometry-optimized triplet isomer **2** ( $^3A$ ).

Along the reaction coordinate for H-migration that connects **1** and **2**, we did not find an additional minimum on the quintet potential-energy hypersurface. Instead, the transition structure TS **1/2** ( $^5A$ ) for a  $\beta$ -hydrogen transfer from the methyl group to the iron center could be located. The optimized geometry (Figure 5) displays a C-O bond length of 1.29 Å which is in between the values for C-O single and double bonds. As compared to **1**, the Fe-O bond in TS **1/2** ( $^5A$ ) is elongated from 1.70 to 1.90 Å and the Fe-H bond (1.67 Å) is already quite short.  $r_{\text{C-H}}$  is fairly large (1.90 Å), pointing to a more advanced formation of the Fe-H bond than the breaking of the Fe-O bond in the TS. The participation of the heavy atoms

(45) Both structures exhibit very small imaginary frequencies for the rotational modes of the methyl group of  $i20\text{ cm}^{-1}$  and  $i34\text{ cm}^{-1}$ , respectively.

(46) The theoretical accuracy includes the possibility that these structures are truly linear. As noted in the Computational Details section, the calculations were performed in  $C_1$  symmetry in order to avoid problems encountered at higher symmetries.

(47) Geometry of isolated  $\text{H}_3\text{CO}^\bullet$  ( $^2E$ ) with Becke3LYP:  $r_{\text{C-O}} = 1.38$  Å,  $r_{\text{C-H}} = 1.11$  Å,  $\alpha_{\text{O-C-H}} = 111^\circ$ .

(48) Ziegler, T.; Li, J. *Can. J. Chem.* **1994**, *72*, 783.

(49) (a) Langhoff, S. R.; Bauschlicher, C. W., Jr. *Annu. Rev. Phys. Chem.* **1988**, *39*, 181. (b) Sodupe, M.; Lluch, J. M.; Oliva, A.; Illas, F.; Rubio, J. *J. Chem. Phys.* **1989**, *90*, 6436. (c) McKee, M. L. *J. Am. Chem. Soc.* **1990**, *112*, 2601. (d) Ohanessian, G.; Goddard, W. A., III *Acc. Chem. Res.* **1990**, *23*, 386.

(50) Geometry of isolated  $\text{H}_2\text{CO}$  ( $^1A_1$ ) with Becke3LYP:  $r_{\text{C-O}} = 1.21$  Å,  $r_{\text{C-H}} = 1.11$  Å,  $\alpha_{\text{O-C-H}} = 122^\circ$ .  $\text{FeH}^+$  ( $^5\Delta$ ):  $r_{\text{Fe-H}} = 1.58$  Å.

(51) Depending on the numerical grid used in geometry optimization, **2** ( $^5A_2$ ) is slightly disturbed out of  $C_{2v}$  symmetry. However, for the most accurate grid, these deviations are within the convergence thresholds of the optimization.

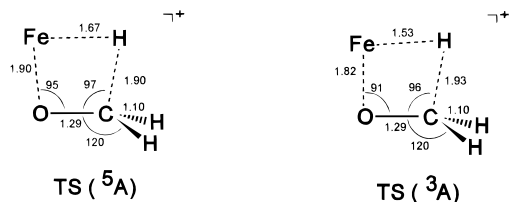


Figure 5. Structures of TS 1/2 ( $^5A$ ) and TS 1/2 ( $^3A$ ).

along the mode of the H migration is reflected by the relatively small imaginary frequency of  $i668\text{ cm}^{-1}$ . Energetically, TS 1/2 ( $^5A$ ) is located 37 kcal/mol above **1** ( $^5A''$ ) and 28 kcal/mol above **2** ( $^5A_2$ ), 33 and 27 kcal/mol, respectively, after ZPVE effects are considered. These results are in accord with the experimental implications that the barrier for the unimolecular  $\beta$ -H transfer  $\mathbf{1} \rightleftharpoons \mathbf{2}$  is quite substantial and that its energy demand is not significantly lower than that for loss of formaldehyde from **2**. Hence, the calculations suggest that a unimolecular interconversion between vibrationally cold **1** and **2** is not very likely to occur.

These computational findings are indeed quite different from the situation in the  $\text{HCo}(\text{CH}_2\text{O})(\text{CO})_3 \rightleftharpoons \text{Co}(\text{OCH}_3)(\text{CO})_3$  system studied earlier by Versluis and Ziegler.<sup>5</sup> These authors reported a negligible barrier for H-C bond formation and the involvement of a second species in the interconversion process that was assigned as a  $\beta$ -agostic minimum. What is the origin of this qualitative difference between the closed-shell  $\text{Co}(\text{OCH}_3)(\text{CO})_3$  system and the open-shell  $\text{Fe}(\text{OCH}_3)^+$  species? To answer this question, we first have to consider the electronic requirements for agostic interaction. As expected and in accord with our calculations in the  $[\text{Fe}, \text{C}, \text{H}_3, \text{O}]^+$  system, the reactant and product possess (high-spin) quintet ground states. In **1**, the covalent Fe-O bond is realized through spin-coupling between the methoxy radical and the singly-occupied 4s orbital of  $\text{Fe}^+$ , while the remaining d-electrons on the iron center are high-spin coupled to maximize exchange energy. Consequently, in the quintet ground state the low-lying orbitals are all singly or doubly occupied, such that donation of electron density to the iron center in an agostic interaction has to involve the antibonding 4s-like orbital and is hampered by three- and four-electron repulsions. In contrast, the (low-spin) triplet states bear low-lying unoccupied acceptor orbitals, which could experience a considerable stabilization through  $\beta$ -agostic interactions. Indeed, the triplet PES is much flatter and TS 1/2 ( $^3A$ ) is located only 8 kcal/mol above the corresponding quintet TS 1/2 ( $^5A$ ).<sup>52</sup> Although the optimized geometry of TS 1/2 ( $^3A$ ) displays qualitatively similar features as discussed for TS 1/2 ( $^5A$ ), it is in general more compact. For example, the Fe-O and Fe-H bond formations are more advanced, and the imaginary frequency of  $i376\text{ cm}^{-1}$  is quite small, which coincides with the qualitative description outlined above for the low-spin TS. However, despite this favorable structure of the triplet TS, its energy is still too high to account for a facile isomerization  $\mathbf{1} \rightleftharpoons \mathbf{2}$  via curve crossing to the low-spin surface (Figure 6).<sup>53</sup>

(52) In order to confirm the accuracy of the DFT approach with respect to the splitting between the triplet and the quintet surface, we performed CCSD(T) calculations for the crucial species TS 1/2 ( $^5A$ ) and TS 1/2 ( $^3A$ ) using the Becke3LYP-optimized geometries. These CCSD(T) calculations were also performed with GAUSSIAN92/DFT and the same basis sets were used, except for one additional f-function (three-term fit to a Slater-type orbital) for iron. At this level of theory, the energy difference between the high- and the low-spin TS is even higher, 15 kcal/mol as compared to 8 kcal/mol with Becke3LYP. In view of the limited accuracy of both approaches, this qualitative agreement justifies the use of the economic hybrid method.

(53) (a) Fiedler, A.; Schröder, D.; Shaik, S.; Schwarz, H. *J. Am. Chem. Soc.* **1994**, *116*, 10734. (b) Shaik, S.; Danovich, D.; Fiedler, A.; Schröder, D.; Schwarz, H. *Helv. Chim. Acta* **1995**, *78*, 1393.

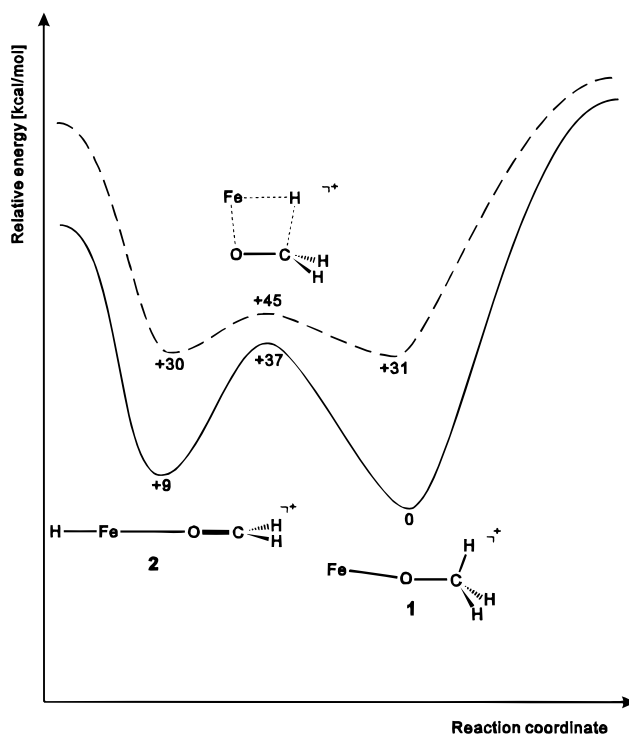


Figure 6. Calculated potential-energy hypersurface for  $\beta$ -hydrogen transfer connecting isomers **1** and **2** on the quintet (full line) and triplet (dashed line) surfaces.

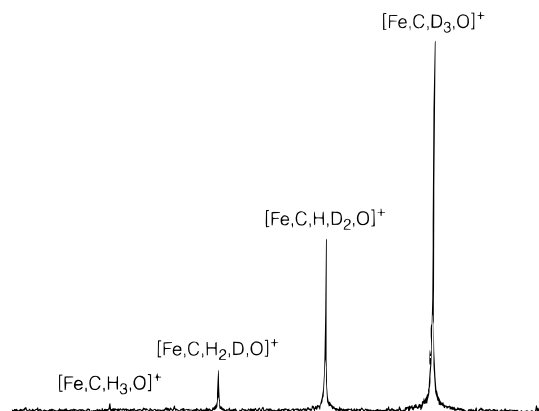


Figure 7. H/D exchange in the ion/molecule reaction of  $[\text{Fe}, \text{C}, \text{D}_3, \text{O}]^+$  with ethene; reaction time 5 s at a partial pressure of ethene of ca.  $2 \times 10^{-8}$  mbar.

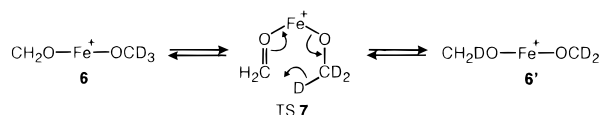
**Reactivity.** Reactivity studies of iron alkoxide cations have been reported in a series of previous articles.<sup>12,14,44</sup> Here, we would like to focus on three representative reactions of  $[\text{D}_3]$ -labeled **1** and/or **2**, i.e. with ethene, water, and formaldehyde. For this purpose,  $[\text{Fe}, \text{C}, \text{D}_3, \text{O}]^+$  ions were generated in the FTICR by reacting bare  $\text{Fe}^+$  with a pulsed-in ca. 1:200 mixture of  $\text{CD}_3\text{NO}_2$  and argon. The latter gas was used for ion thermalization (overall ca. 500 collisions). Note, that according to the thermochemistry determined here the reaction of  $\text{Fe}^+$  with nitromethane allows for the formation of isomers **1** as well as **2** ( $\Delta_R H = -25$  and  $-10$  kcal/mol, respectively), which may then be thermalized by the argon buffer gas.

When so-formed  $[\text{Fe}, \text{C}, \text{D}_3, \text{O}]^+$  ions are allowed to react with ethene, H/D exchange (Figure 7) is observed exclusively, and  $[\text{Fe}, \text{C}, \text{H}_3, \text{O}]^+$  is formed as the terminal reaction product. No  $\text{FeC}_2\text{H}_{4-n}\text{D}_n^+$  ( $n = 0-4$ ) isotopologues are formed. Mechanistically, H/D exchange can easily be rationalized by reversible  $\beta$ -hydrogen transfer from **2** via  $(\text{C}_2\text{H}_4)\text{Fe}(\text{D})(\text{OCD}_2)^+$  as a possible intermediate. The fact that in the course of the reaction



**Ligand Effects.** As demonstrated above the unimolecular interconversion  $\mathbf{1} \rightleftharpoons \mathbf{2}$  is associated with a substantial barrier,

Scheme 4



but the interconversion is facilitated in the presence of additional ligands (e.g. ethene or formaldehyde). What are possible origins of these ligand effects? We first note that each additional ligand will increase the splitting of the d-orbitals of iron, thus stabilizing the low-spin configurations relative to the high-spin surfaces. Because the barrier associated with  $\beta$ -hydrogen transfer is not very high on the low-spin surface, the triplet potential-energy hypersurface may fall below the quintet potential-energy hypersurface and the path with the lowest energy demand will involve a triplet **TS** together with two curve crossings.<sup>53b</sup> If so, then the interconversion  $\mathbf{1} \rightleftharpoons \mathbf{2}$  becomes more likely as more ligands are present in the encounter complex. Eventually this reasoning leads to very low barriers for situations similar to that proposed by Versluis and Ziegler<sup>5</sup> for the 18-electron species  $\text{HCO}(\text{CO})_3(\text{CH}_2\text{O})$ . Nevertheless, a single ligand such as water, ethene, or formaldehyde is not likely to lower the barrier for interconversion of **1** and **2** enough that unimolecular isomerization becomes rapid.

There is an alternative mechanism for the H/D equilibration described in Figure 8 and Scheme 3, in which the ligand does not merely serve as a spectator, but is actively involved in bond formation (Scheme 4).<sup>54</sup> This mechanism is attractive because it proceeds via the six-membered transition structure **TS 7** and does not involve an energetically less favored iron hydride intermediate analogous to **2**. A similar situation may prevail in the  $[\text{Fe}, \text{C}, \text{D}_3, \text{O}]/\text{C}_2\text{H}_4^+$  complex. However, in the case of reaction 4, the water ligand, which lacks a double bond, is not capable of covalently binding another hydrogen (deuterium).

(54) Becker, H.; Schröder, D.; Zummack, W.; Schwarz, H. *J. Am. Chem. Soc.* **1994**, *116*, 1096.

Therefore, neither interconversion of **1** and **2** nor H/D exchange processes should be apparent in the reaction with water, as observed experimentally.

Conclusions

The combined mass spectrometric and computational studies reported here have several implications. First, the methods of ion generation in different kinds of mass spectrometers do not necessarily lead to the same species. In the present case, most of the methods for ion generation lead to mixtures of  $\text{Fe}(\text{OCH}_3)^+$  and  $\text{HFe}(\text{OCH}_2)^+$ , because *intermolecular* isomerization is facile, although the barrier for *intramolecular* rearrangement is relatively large. Thus, even though these ions may be thermalized by collisional cooling techniques, distinct isomers may be trapped in their potential wells if the corresponding barriers for their interconversions are sufficiently high, as in the present case. Second, the computations reveal that the low-spin (possibly excited) surfaces for d-block elements may be attractive pathways for the transition structures of a particular rearrangement, because they meet the conditions of donor–acceptor interactions of empty and filled orbitals in the metal and the ligand. Third, the present study underlines the effect of additional ligands on a transition-metal center, in particular, when the ligands are actively involved in the reaction coordinate. Finally, the present findings reveal that even in small compounds such as  $\text{Fe}(\text{OCH}_3)^+$ , the mechanism of  $\beta$ -hydrogen transfer is not simple and subtle ligand effects and curve crossings may play a role.

**Acknowledgment.** The Berlin group acknowledges continuous financial support by the Deutsche Forschungsgemeinschaft, the Volkswagen Stiftung, and the Fonds der Chemischen Industrie. The Utah group has been supported by the National Science Foundation, Grant CHE-9221241. D.S. thanks the Deutsche Forschungsgemeinschaft and the Auswärtiges Amt for a travel grant which helped initiate this collaborative effort.

JA953039Q